REPORT

POLYMERS

Random heteropolymers preserve protein function in foreign environments

Brian Panganiban,[1] Baofu Qiao,[2] Tao Jiang,[1] Christopher DelRe,[1] Mona M. Obadia,[3] Trung Dac Nguyen,[2] Anton A. A. Smith,[1] Aaron Hall,[1] Izaac Sit,[1] Marquise G. Crosby,[4] Patrick B. Dennis,[4] Eric Drockenmuller,[3] Monica Olvera de la Cruz,[2,5] Ting Xu[1,6,7,8]*

The successful incorporation of active proteins into synthetic polymers could lead to a new class of materials with functions found only in living systems. However, proteins rarely function under the conditions suitable for polymer processing. On the basis of an analysis of trends in protein sequences and characteristic chemical patterns on protein surfaces, we designed four-monomer random heteropolymers to mimic intrinsically disordered proteins for protein solubilization and stabilization in non-native environments. The heteropolymers, with optimized composition and statistical monomer distribution, enable cell-free synthesis of membrane proteins with proper protein folding for transport and enzyme-containing plastics for toxin bioremediation. Controlling the statistical monomer distribution in a heteropolymer, rather than the specific monomer sequence, affords a new strategy to interface with biological systems for protein-based biomaterials.

Nature's building blocks, such as proteins and biomachinery, have many features unmatched by synthetic counterparts, including chemical diversity, hierarchical structure, programmed system dynamics, and efficient energy conversion. Despite years of effort to stabilize proteins outside of their native environments, there has been limited development in interfacing biological and synthetic components without compromising their structures and inherent functions. Nonaqueous enzymology via reverse micelles can only maintain a fraction (<20%) of native activity (*1*); amphipols solubilize membrane proteins, but not for water-soluble proteins in organic solvents (*2*); polymer conjugation relies on accessibility of protein-functional groups (*3*); and sol-gel confinement limits protein accessibility and postintegration (*4*).

A chaperone-like polymeric shell outside of a protein may effectively improve protein solubility and stability in organic solvents by providing a barrier to resist both organic solvent exposure and protein conformational change. To form such a nanoscopic polymeric shell, protein-polymer interactions need to be strong enough to favor adsorption yet soft enough not to outcompete the forces governing protein folding. The structure and activity of natural building blocks are governed by multiple noncovalent interactions that are subject to change with small perturbations (*5*). When a homopolymer is conjugated to a protein surface, monomer–amino acid interactions can affect protein folding (*6*, *7*) and deform the polymer chain conformation (*8*). In nature, intrinsically disordered proteins adopt local chain conformations, often achieved by multiple weak binding sites, and mediate various processes (*9*, *10*). Amphiphilic heteropolymers mimicking disordered proteins may offer a versatile approach for protein solubilization and stabilization given, the diversity and complexity of proteins.

Protein surfaces are chemically diverse and heterogeneous (Fig. 1A). Surface analysis of folded water-soluble proteins based on hydrophobicity or charge shows characteristic patch size distributions. The typical patch size is 1 to 2 nm in diameter, with an interpatch distance of 1 to 2 nm (Fig. 1B and fig. S1). Sequence analysis of water-soluble proteins, performed by assigning amino acids as either hydrophilic or hydrophobic, using glycine as the reference (*11*), shows that the block length of amino acids with similar hydrophobicity tends to be less than 10 (fig. S2). Matching the statistical chemical pattern has been shown to be critical in de novo protein design (*12*, *13*) and in modulating polymer/surface interactions (*14*). Rather than synthesizing sequence-specific polymers (*15*), synthetic heteropolymers with similar chemical features and spatial distributions of side chains to match the surface pattern of natural proteins may behave like disordered proteins.

Recent developments in reversible deactivation radical polymerization make it feasible to synthesize random heteropolymers with reliable control over the statistical monomer distribution (*16*–*18*). Four methacrylate-based monomers are selected to impart chemical diversity in heteropolymers and to optimize short-range polymer-protein interactions (Fig. 1C and fig. S3): methyl methacrylate (MMA), oligo(ethylene glycol) methacrylate [OEGMA; number-average molecular weight (M_n) = 500 Da], 2-ethylhexyl methacrylate (2-EHMA), and 3-sulfopropyl methacrylate potassium salt (3-SPMA). MMA is chosen to tailor the overall hydrophobicity for protein solubilization, to anchor the chain at the polar-nonpolar interface, and to reduce the entropic penalty associated with adjusting its local conformation. OEGMA is chosen to leverage the well-known ability of poly(ethylene glycol) (PEG) to stabilize proteins. 2-EHMA and 3-SPMA are chosen to interact with the hydrophobic and positively charged residues on the protein surface, respectively. The selection of the monomer ratio is guided by the calculated solubility parameters (*19*, *20*) and through experimental screenings to achieve polymer dispersion in both aqueous and organic media with the best retention in enzyme activity. Our best-performing heteropolymer, called "RHP," has a compositional ratio of 5(MMA):2.5(OEGMA):2(2-EHMA):0.5(3-SPMA). Using the well-established Mayo-Lewis equation, we estimated the statistical monomer distribution along the RHP chains (*21*, *22*). The histogram of monomer block size confirms the absence of long blocks of the same monomer that could interfere with native protein structure (figs. S5 to S7). The RHP used has a M_n of ~30 kDa and a dispersity of 1.3. At least 12 batches of RHP were synthesized with excellent reproducibility (fig. S11).

Computational studies were performed on mixtures of a common enzyme, horseradish peroxide (HRP), and RHP in both an aqueous buffer solution and toluene in order to elucidate the polymer-protein adsorption mechanism. Explicit solvent all-atom molecular dynamics (MD) simulations were performed by using the CHARMM 36 potential (supplementary materials, section S3). The RHPs are built with compositions and degrees of polymerization close to the corresponding experimental values. The last simulation snapshots of the RHP/HRP mixture in toluene and in water are shown in Fig. 2, A and B, respectively. In water, RHP and HRP are loosely complexed, and only ~40% of HRP surface is covered by RHP, which is in line with the experimental observations that RHP is soluble in water. However, the HRP surface is fully covered by RHPs in toluene; the complex is stable, and no protein structure change was observed over the simulation duration of 0.6 μs. The radial distribution of RHPs around the protein's center of mass was calculated in toluene (Fig. 2C) and in water (fig. S17E). In toluene, the hydrophilic monomers of the polymer (OEGMA and 3-SPMA) were found to

[1]Department of Materials Science and Engineering, University of California, Berkeley, Berkeley, CA 94720, USA. [2]Department of Materials Science and Engineering, Northwestern University, Evanston, IL 60208, USA. [3]Université Lyon, Université Lyon 1, CNRS, Ingénierie des Matériaux Polymères, UMR 5223, F-69003 Lyon, France. [4]Air Force Research Laboratory, Wright-Patterson Air Force Base, OH 45433, USA. [5]Department of Chemistry, Northwestern University, Evanston, IL 60208, USA. [6]Department of Chemistry, University of California, Berkeley, Berkeley, CA 94720, USA. [7]Materials Science Division, Lawrence Berkeley National Laboratory, Berkeley, CA 94720, USA. [8]Tsinghua-Berkeley Shenzhen Institute, University of California, Berkeley, Berkeley, CA 94720, USA.
*Corresponding author. Email: tingxu@berkeley.edu

point inward, adjacent to the protein, whereas the hydrophobic monomers (MMA and 2-EHMA) were located on the outside, in contact with the toluene. By contrast, the favored orientations of the RHP side chains become weaker in water. These results suggest that once positioned close to the protein surface, the RHPs can adjust their conformations to maximize protein-polymer interactions, which correlates well with our hypothesis. Correlations between the protein surface groups and their nearest monomer neighbors are computed by categorizing Ala, Val, Ile, Leu, Met, Phe, Tyr, Trp, Gly, and Pro amino acids as hydrophobic and the others as hydrophilic. Approximately 70% of the protein surface is covered by the hydrophilic monomers; 50 ± 4% originates from hydrophilic monomer–hydrophilic amino acid interactions, contributing –800 ± 300 kJ/mol to the energy (Fig. 2D). This shows the importance of the local protein surface-polymer interactions in stabilizing the protein structure. The shell formed by the polymer around the HRP core in organic solvents improves protein solubility and stability by providing a barrier to resist both organic solvent exposure and protein conformational change.

The role of the RHPs' composition on their ability to encapsulate the protein in water and toluene was investigated by using a coarse-grained (CG) model based on the data gathered from all-atom MD simulations and experiments (Fig. 2E and supplementary materials, section S4). A representative snapshot of the RHP encapsulating the protein is given in Fig. 2F. The surface coverage increases as the attraction strength between the adsorbing monomers and protein-attractive sites, ε_{Hh}, increases (Fig. 2G) for all solvent selectivity conditions (captured by the attraction strength between the polymer solvophobic beads, ε_{hh}). For sufficiently high ε_{hh}, there exists an optimal value of the fraction of adsorbed monomers (ϕ_A) that maximizes the surface coverage (Fig. 2H). The spatial correlations between the adsorbing monomers and the protein-attractive sites (fig. S22A) demonstrate that the RHPs tend to adopt energetically favored conformations once in contact with the protein to compensate for the entropic penalty associated with confinement to the surface (*23*).

We experimentally tested our hypothesis that RHP is capable of interacting with proteins and mediating their interactions with the local environment. We performed cell-free synthesis of membrane proteins that eliminates potential interference or assistance from the host cell physiology for protein folding and lipid insertion during translation (*24*). Once the plasmids for a model transmembrane protein—oligopeptide/proton symporter PepTso or water channel aquaporin Z (AqpZ)—are added, the translation and folding status of the membrane protein is scored according to the fluorescence intensity of a C terminus–fused green fluorescent protein (GFP). Western blotting analysis (Fig. 3A) using antibodies to GFP confirmed PepTso-GFP expression regardless of the presence of RHP. Without RHP, no GFP fluorescence is detected, suggesting that protein folding is not correct to gain GFP fluorescence (*25*). Control experiments using amphipol (A8-*35*), which is effective in stabilizing membrane proteins after protein expression, show little GFP fluorescence for AqpZ-GFP (*2*). However, there is a ~15-fold increase in GFP fluorescence when PepTso-GFP or AqpZ-GFP is expressed in the presence of RHP at a RHP:ribosome mole ratio of 50:1 (Fig. 3B). The resultant GFP fluorescence is more than an order of magnitude higher than that of commonly used liposome. To further verify the protein folding, the cell-free synthesized PepTso was reconstituted in liposomes and tested in a pyranine-based proton transport assay (Fig. 3C) (*26*). Proton transport was detected by adding valinomycin to the outer solution containing a dipeptide, Ala-Ala (Fig. 3D). The cell-free synthesized PepTso, in the presence of RHP, can fold properly to retain transport function in a lipid environment. Thus, RHP is able to chaperone proper protein folding and solubilize membrane proteins in aqueous solution but will not outcompete the protein-lipid interaction, interfere with lipid insertion, or compromise transport function.

We investigated protein dispersion and stabilization in organic solvents, a requirement to interface proteins with synthetic building blocks toward protein-based materials. Previous nonaqueous enzymology studies of HRP observed only less than 1% of its native activity in hydrophobic solvents that can extract the heme cofactor (*27*). For all studies, proteins and RHPs were first cosolubilized in deionized water, lyophilized, and subsequently resuspended in solvents.

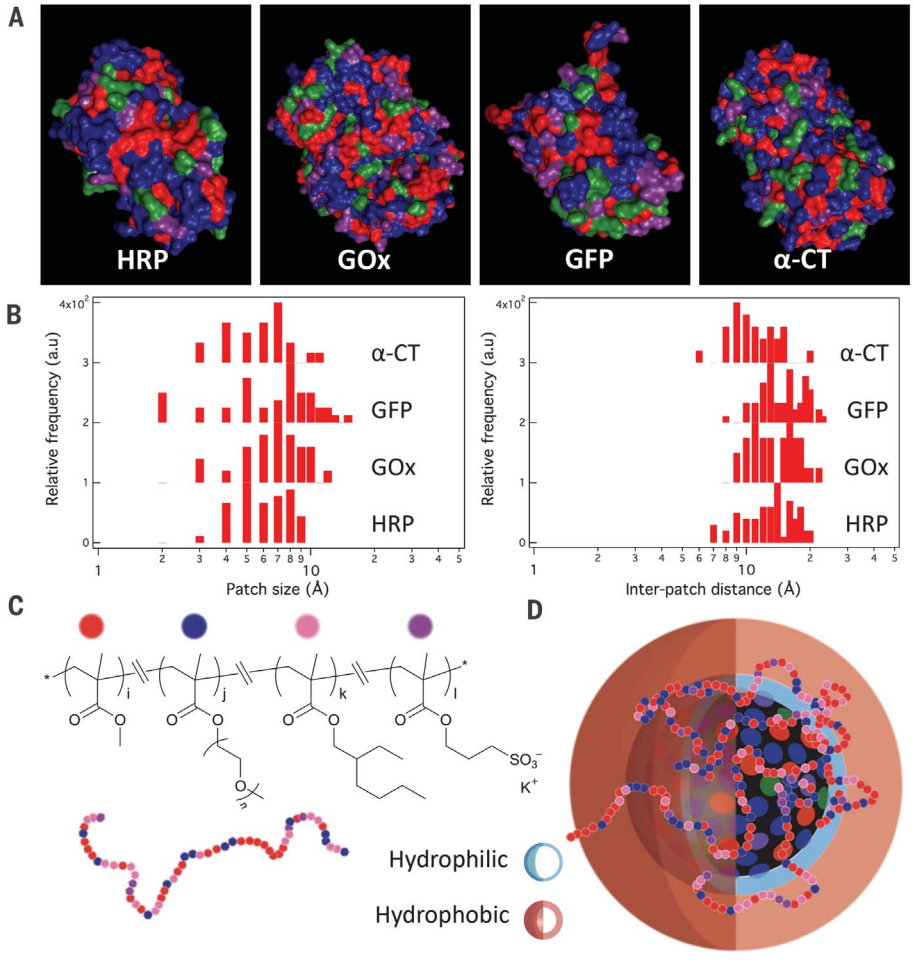

Fig. 1. Design of random heteropolymers based on protein surface pattern for protein solubilization and stabilization in organic solvents. (**A**) As seen in the color-coded proteins—HRP(1H55), GOx(1CF3), GFP(2HRW), and α-CT(1YPH)—the protein surfaces are chemically heterogeneous, with characteristic patch size and interpatch distance. Neutral hydrophilic, blue; hydrophobic, red; positively charged, green; negatively charged, purple. (**B**) The histograms of the patch diameter and the interpatch distance show that the length centers around 1 to 2 nm. Analysis of hydrophobic patches is shown. Analysis of negatively and positively charged patches is shown in fig. S1. (**C**) Designed random heteropolymer with statistical distribution of monomers with varied hydrophobicity matching that of the protein. (**D**) The RHP can coassemble with protein (schematically shown as a patchy particle) in organic media in which the random heteropolymer adjusts its local conformation to maximize protein-heteropolymer interaction without denaturing the protein's local structure.

The RHP/HRP complexes were readily soluble in common solvents for material synthesis and processing such as toluene and chloroform. Transmission electron microscopy (TEM) results (Fig. 4A) show that RHP/HRP complexes form nanoparticles with a diameter of ~50 to 60 nm. Fourier transform-infrared spectroscopy (FTIR) spectra were collected after dissolving RHP/HRP complexes in toluene over 24 hours. The amide I band and its corresponding negative second derivative revealed minimal change in the HRP's secondary structure in toluene (Fig. 4B). There is little change (<2 nm) in the peak position in the ultraviolet (UV)–visible spectra of the heme cofactor in HRP over 24 hours (Fig. 4C),

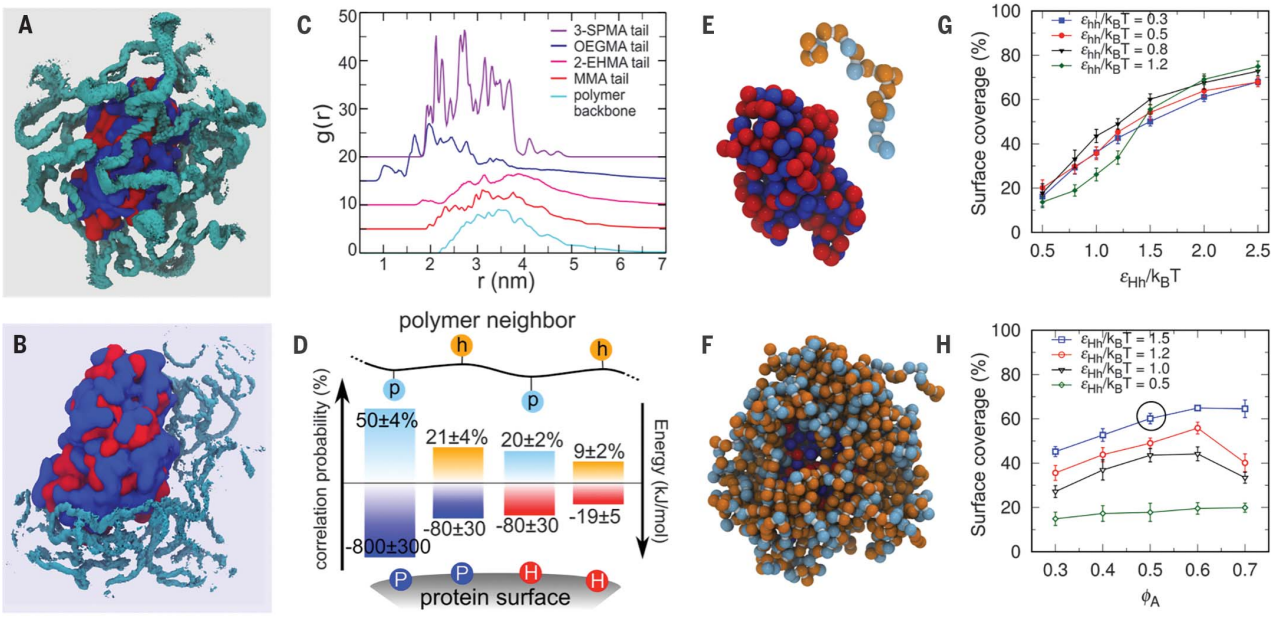

Fig. 2. All-atom and CG molecular dynamics simulation results. (**A** and **B**) Three-dimensional spatial distribution of polymer backbone (cyan) around HRP in (A) toluene and (B) water. The isosurfaces are plotted for densities 50 times the average. The hydrophilic and hydrophobic protein surfaces are colored in blue and red, respectively. (**C**) Radial density profiles of the polymer backbone and the tail atoms of the four monomers (fig. S12) around the center of mass of HRP backbone in toluene. (**D**) Correlation probability (in percent) and energy (kilojoule per mole) between the hydrophilic (P, blue) and hydrophobic (H, red) protein surface and the hydrophilic (p, light blue) and hydrophobic (h, orange) polymer nearest neighbors in toluene. The uncertainties refer to the standard deviations. (**E**) CG models of HRP and a RHP chain, where the red beads represent the protein-attractive sites and the orange beads represent the adsorbing monomers. (**F**) A snapshot of the RHP chains covering the HRP. (**G**) The surface coverage as a function of the adsorption strength. (**H**) The surface coverage as a function of the MMA composition. An example of the system corresponding to the circled data point is illustrated in (F).

Fig. 3. Random heteropolymers can effectively mediate interaction between membrane protein and aqueous solution and assist protein folding during translation in cell-free synthesis. (**A**) Western blot analysis of protein expression with and without RHP in a cell-free synthesis assay. The left lane shows color-coded protein mass standards. (**B**) The level of proper protein folding of GFP-fused AqpZ is significantly enhanced with the presence of RHP (n = 3 independent measurements) in comparison with other surfactants, such as amphipol A8-35 and dioleoylphosphatidylcholine (DOPC) unilamellar liposome. (**C**) Schematics of assay to evaluate PepTso transport properties upon insertion into liposomes. (**D**) Cell-free synthesized PepTso in the presence of RHP can fold and inset into lipids properly, retaining transport function across the membrane.

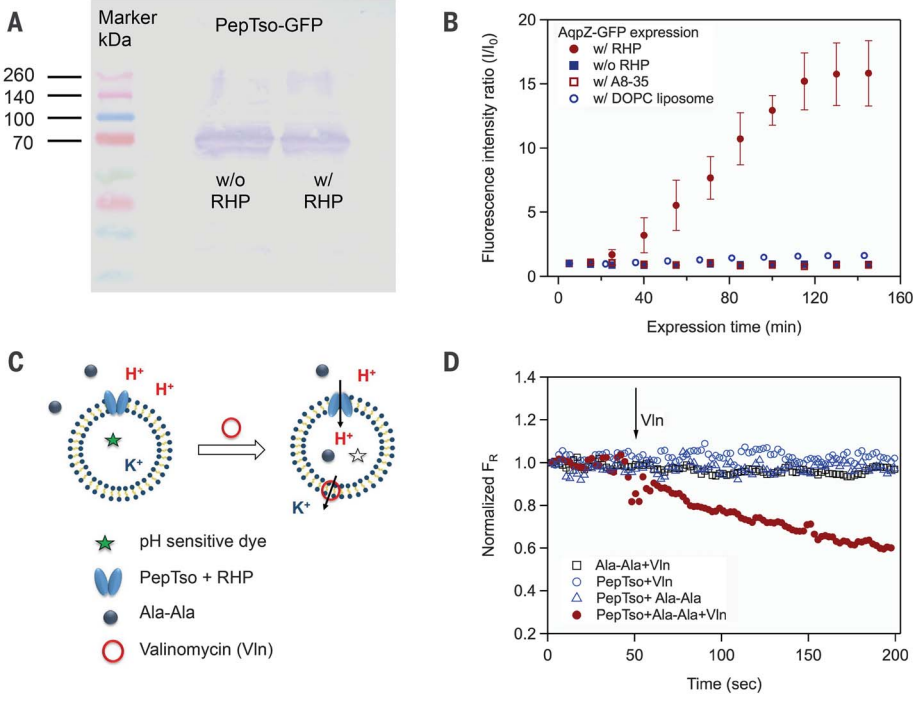

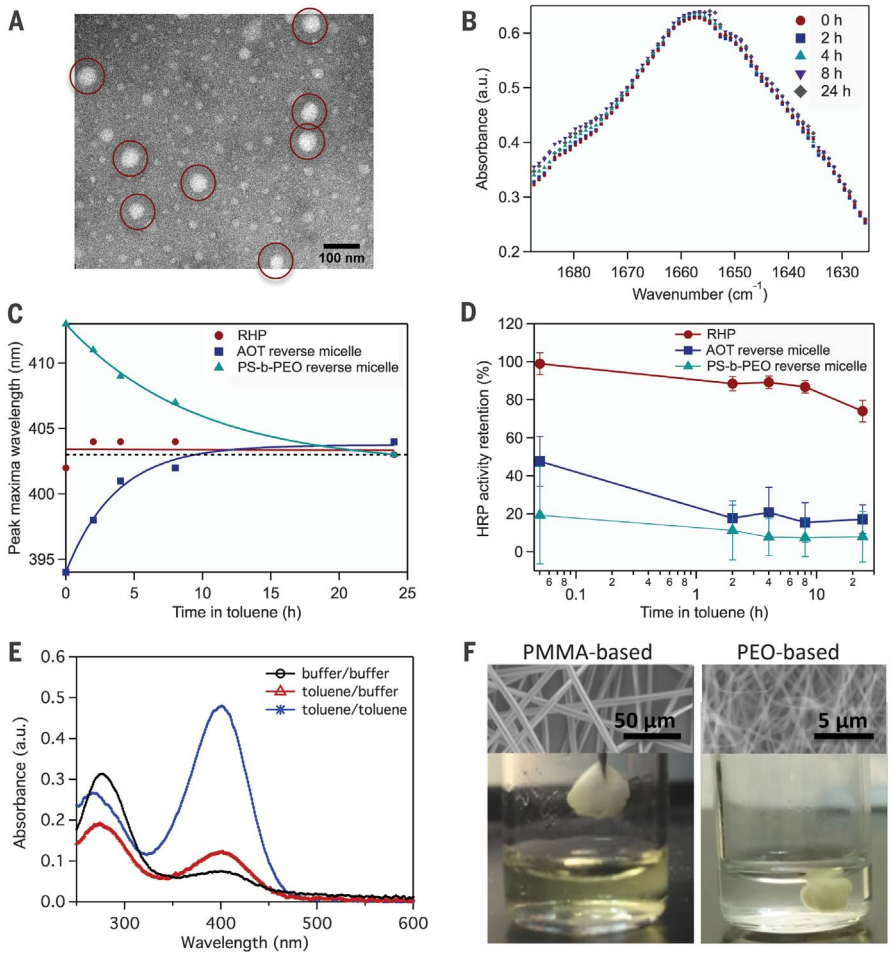

Fig. 4. Random heteropolymers preserve enzymes in organic solvents and enable processing of protein-containing functional materials. (**A**) TEM image of RHP/HRP dried from toluene solution. The RHP/HRP mixture forms ~50- to 60-nm-diameter nanoparticles (red circles). (**B**) FTIR spectra of the RHP/HRP complex in toluene over 24 hours, suggesting minimal changes in the protein secondary structure. (**C**) The peak position of the UV-visible spectrum of the heme cofactor in RHP/HRP complex in toluene over 24 hours, confirming the integrity of its protein tertiary structure and enzymatic pocket. (**D**) In the presence of RHP, ~80% of native HRP activity is retained after being stored in toluene over 24 hours (n = 3 independent measurements). Results from HRP encapsulated in reverse micelles based on sodium bis(2-ethylhexyl) sulfosuccinate (AOT) (<25%) or polystyrene-block-poly(ethylene oxide) (PS-*b*-PEO) polymeric surfactant (<18%) are shown for comparison. (**E**) Enzymatic activity of OPH as a function of storage media for OPH and substrate. Activity seven times higher than control experiments in buffer can be obtained when OPH and the pesticide methyl parathion are cosolubilized in toluene. (**F**) Electrospun PEO- or PMMA-based fiber mats containing RHP/OPH complex can perform on-demand bioremediation. The hydrolysis by-products are trapped in the RHP/OPH/PEO fiber mat for easy removal.

confirming the retention of HRP tertiary structure and stability of the heme-binding pocket in toluene, which is critical for enzymatic activity. To evaluate the retention of the HRP activity after suspension in toluene, aliquots of RHP/HRP toluene solution were dispersed in aqueous solution in order to perform a colorimetric assay. With the presence of RHP, ~80% of HRP native activity was maintained after 24 hours suspended in toluene (Fig. 4D). This is several orders of magnitude higher than HRP alone in nonaqueous media and at least four times higher than the best reported value when using molecular and/or polymeric surfactants (*1*).

We explored the versatility and universality of RHP by extending the study to other proteins. PEGylation is effective for protein dispersion and stabilization but is not effective for proteins with a small number of functionalizable groups, such as glucose oxidase (GOx) (*28*). (fig. S24). The PEGylation is sufficient for GOx dispersion, but the proteins retain less than 10% of native activity after 2 hours (fig. S24). By contrast, RHP/GOx shows ~50% of native activity after 24 hours of storage in toluene. Proteins with different structures, such as β-barrel GFP, are also tested. After RHP/GFP complex is solubilized in organic solvents, there is no detectable shift in fluorescent emission peak maxima and minimal decrease in the emitted fluorescence over 24 hours (fig. S25). These results confirm that the environment in the β-barrel interior remains the same and suggest that there is minimal toluene penetration into the protein core.

The RHP-enabled protein solubilization and stabilization can lead to technologically relevant protein-based materials. Organophosphorus hydrolase (OPH) was chosen for its excellent ability to degrade organophosphates, which are commonly used as insecticides and chemical warfare agents (*29*). However, OPH becomes inactive even in its partially folded dimeric state (*30*), and organophosphates typically have poor solubility in aqueous solution. There is a need to retain OPH activity while cosolubilized with organophosphates in order to realize on-demand bioremediation for these acute toxins. We evaluated OPH activity using a 10 mM preparation of the well-known pesticide methyl parathion (MP). RHP/OPH can be readily solubilized in toluene and chloroform and resuspended in buffer solution. RHP/OPH retains 80 ± 5.6% (n = 3 independent measurements) of the initial OPH activity after 24 hours' suspension in toluene. When methyl parathion was codissolved with RHP/OPH in toluene, dried, and assayed, the OPH activity was more than seven times higher than that of pure OPH in aqueous solution (Fig. 4E). This is attributed to the higher substrate concentration in toluene and RHP's ability to stabilize OPH in both aqueous and organic media. The successful dispersion and stabilization of RHP/OPH complexes enables coprocessing of OPH and synthetic polymers (Fig. 4F). Fiber mats based on either polyethylene oxide (PEO) or PMMA were prepared by means of electrospinning and tested for bioremediation. Both fiber mats were active and degraded MP, weighing approximately 1/10 of the total fiber mat, in a few minutes. In particular, when the RHP/OPH/PEO fiber mat was soaked in MP-containing toluene solution and assayed in buffer, the hydrolysis by-products could be trapped for easy removal. This enables in situ toxin remediation without preprocessing, transfer, or contact with the agent before and after detoxification.

Our studies confirm that random heteropolymers designed on the basis of statistical monomer distribution are effective at maintaining protein function in foreign environments. Using only one design of random heteropolymer, we demonstrated successful cell-free synthesis of membrane proteins with proper folding and retention of protein activity in organic solvents for a wide range of proteins. These hybrid materials will not only take advantage of the precision and efficiency of natural building blocks but also enable reactions and processes on demand where common chemistry necessities are unavailable.

REFERENCES AND NOTES

1. A. M. Klibanov, *Nature* **409**, 241–246 (2001).
2. J.-L. Popot *et al.*, *Cell. Mol. Life Sci.* **60**, 1559–1574 (2003).
3. E. M. Pelegri-O'Day, H. D. Maynard, *Acc. Chem. Res.* **49**, 1777–1785 (2016).

4. R. B. Bhatia, C. J. Brinker, A. K. Gupta, A. K. Singh, *Chem. Mater.* **12**, 2434–2441 (2000).
5. K. A. Dill, *Biochemistry* **29**, 7133–7155 (1990).
6. J. Y. Shu *et al*., *Biomacromolecules* **11**, 1443–1452 (2010).
7. N. Dube, A. D. Presley, J. Y. Shu, T. Xu, *Macromol. Rapid Commun.* **32**, 344–353 (2011).
8. R. Lund, J. Shu, T. Xu, *Macromolecules* **46**, 1625–1632 (2013).
9. H. J. Dyson, P. E. Wright, *Nat. Rev. Mol. Cell Biol.* **6**, 197–208 (2005).
10. Z. Liu, Y. Huang, *Protein Sci.* **23**, 539–550 (2014).
11. O. D. Monera, T. J. Sereda, N. E. Zhou, C. M. Kay, R. S. Hodges, *J. Pept. Sci.* **1**, 319–329 (1995).
12. W. F. DeGrado, C. M. Summa, V. Pavone, F. Nastri, A. Lombardi, *Annu. Rev. Biochem.* **68**, 779–819 (1999).
13. D. A. Moffet, M. H. Hecht, *Chem. Rev.* **101**, 3191–3203 (2001).
14. P. Mansky, Y. Liu, E. Huang, T. P. Russell, C. J. Hawker, *Science* **275**, 1458–1460 (1997).
15. J. F. Lutz, M. Ouchi, D. R. Liu, M. Sawamoto, *Science* **341**, 1238149 (2013).
16. J. Chiefari *et al*., *Macromolecules* **31**, 5559–5562 (1998).
17. G. Moad, E. Rizzardo, S. H. Thang, *Acc. Chem. Res.* **41**, 1133–1142 (2008).
18. A. E. Smith, X. Xu, C. L. McCormick, *Prog. Polym. Sci.* **35**, 45–93 (2010).
19. A. F. M. Barton, *Handbook of Polymer-Liquid Interaction Parameters and Solubility Parameters* (Taylor & Francis, 1990).
20. J. N. Israelachvili, *Intermolecular and Surface Forces* (Elsevier Science, 2015).
21. B. G. Manders, W. Smulders, A. M. Aerdts, A. M. vanHerk, *Macromolecules* **30**, 322–323 (1997).
22. F. R. Mayo, F. M. Lewis, *J. Am. Chem. Soc.* **66**, 1594–1601 (1944).
23. T. Ge, M. Rubinstein, *Macromolecules* **48**, 3788–3801 (2015).
24. D. Schwarz *et al*., *Nat. Protoc.* **2**, 2945–2957 (2007).
25. A. Müller-Lucks, S. Bock, B. Wu, E. Beitz, *PLOS ONE* **7**, e42186 (2012).
26. J. L. Parker, J. A. Mindell, S. Newstead, *eLife* **3**, e04273 (2014).
27. A. M. Klibanov, *Trends Biotechnol.* **15**, 97–101 (1997).
28. A. D. Presley, J. J. Chang, T. Xu, *Soft Matter* **7**, 172–179 (2011).
29. B. K. Singh, A. Walker, *FEMS Microbiol. Rev.* **30**, 428–471 (2006).
30. J. K. Grimsley, J. M. Scholtz, C. N. Pace, J. R. Wild, *Biochemistry* **36**, 14366–14374 (1997).
31. Data are available from the Dryad Digital Repository; https://doi.org/10.5061/dryad.j1pt126.

ACKNOWLEDGMENTS

We thank A. Presley for PEGylated GOx studies and V. Wu for assistance with coding of heteropolymers sequence simulation. **Funding:** The work was supported by the U.S. Department of Defense (DOD), Army Research Office, under contract W911NF-13-1-0232. B.Q., T.D.N., and M.O.C. thank the support of the Department of Energy award DE-FG02-08ER46539 and the Sherman Fairchild Foundation. E.D. acknowledges support from the Auvergne-Rhône-Alpes region. A.A.A.S. was supported by The Danish Council for Independent Research Award DFF–5054-00215. T.X. acknowledges support from Dreyfus foundation via Camille-Dreyfus Teacher-Scholar Award. E.D. and T.X. acknowledge support from the Fulbright foundation. M.O.C. and T.X. acknowledge support from the Miller Institute. C.D. is supported by the DOD through the National Defense Science and Engineering Graduate Fellowship (NDSEG) Program. **Author contributions:** T.X. conceived the idea and guided the project. B.P. performed studies using RHP with HRP, CT, GOx, and GFP. T.J. performed cell-free synthesis of membrane proteins and evaluated their activity. C.D. performed studies using OPH and fabricated and tested the OPH-containing fabrics. B.Q. performed all-atom simulation studies. T.D.N. performed CG simulation studies. B.Q., T.D.N., and M.O.C. analyzed simulation data. E.D. and M.M.O. screened different compositions of RHPs to afford the synthesis and detailed characterization of the first positive hit. A.A.A.S. and A.H. analyzed the RHP monomer distribution, quantified composition drift in RHP, and synthesized different batches of RHPs to verify reproducibility. P.B.D. and M.G.C. provided OPH. All authors participated in writing the manuscript. All authors have no competing interests. **Data and materials availability:** All data needed to evaluate the conclusions in the paper are present in the paper and/or the supplementary materials. For reproduction purposes, raw data used to generate figures are available from the Dryad Digital Repository (https://doi.org/10.5061/dryad.j1pt126) (*31*). Random heteropolymers are available from T.X. under a materials transfer agreement with the University of California, Berkeley. **Competing interests:** T.X., B.P., and T.J. are inventors on a patent application submitted by the University of California, Berkeley, that covers random heteropolymers to preserve proteins in foreign environments.

SUPPLEMENTARY MATERIALS

www.sciencemag.org/content/359/6381/1239/suppl/DC1
Materials and Methods
Figs. S1 to S28
Tables S1 to S4
References (*32*–*52*)
Movies S1 to S2

7 June 2017; accepted 25 January 2018
10.1126/science.aao0335